Honorary Editor: G.E. Brown

# Extension of the Liège intranuclear cascade model at incident energies between 2 and 12 GeV. Aspects of pion production

Sophie Pedoux, Joseph Cugnon *

*University of Liège, AGO Department, allée du 6 Août 17, bât. B5, B-4000 Liège 1, Belgium*

## Abstract

The validity of the standard version of the Liège Intra-Nuclear Cascade (INCL4) model, which has been shown to be quite successful for the description of spallation reactions, is limited to an upper incident energy of ∼2 GeV, because inelastic elementary processes are restricted to the excitation and de-excitation of the Delta resonance. In this paper, the INCL4 model is extended to higher incident energy by including other inelastic elementary collisions. However, excitation of heavier baryonic resonances is replaced by direct multipion production in elementary nucleon–nucleon and pion–nucleon collisions. The predictions of the modified model for production of charged pions by proton and pion beams off nuclei are compared with experimental data of the HARP Collaboration for beam energies between 2 and 12 GeV. The apparent duality between the approach based on excitation of numerous baryonic resonances and our approach is briefly discussed.
© 2011 Elsevier B.V. All rights reserved.

## 1. Introduction

The interest in spallation reactions has recently been revived by the prospect of using Accelerator-Driven Systems (ADS) to incinerate nuclear waste [1]. These devices will use an

---

accelerator to deliver a high-intensity beam of protons on a spallation target, located inside the core of a sub-critical nuclear reactor. Neutrons are expelled from the spallation target, are multiplied in the sub-critical assembly and can be used to transmute nuclear waste: long-lived radioactive isotopes can be transformed into stable or short-lived isotopes. The most promising case seems to be the transmutation of the so-called minor actinides by neutron-induced fission. Neutron production inside the spallation target is the most efficient for proton beams of energy lying in the 1 to 2 GeV range [2]. The design of ADS requires a detailed knowledge of the elementary particle–nucleus interactions. In the last ten years, a strong effort has been made to improve the available models for describing these interactions in the ~100 MeV–~1.6 GeV range. A recent intercomparison of models, organized by the IAEA [3], has shown that the intranuclear cascade model developed at the University of Liège, denoted INCL4 [4], coupled to the evaporation-fission ABLA model of K.-H. Schmidt [5,6], can describe quite well a huge body of experimental data for proton-induced reactions in the 100 MeV–2 GeV range. This includes total reaction cross sections, neutron multiplicities, neutron and proton double differential cross sections, residue mass spectra, isotopic distributions and recoil energies.

Other applications of spallation reactions involve projects of intense neutron spallation sources [7], radiation protection issues regarding cosmic rays in space missions [8] and the development of cancer hadrontherapy over the world [9]. The high predictive power of the INCL4 + ABLA model, combined with its low numerical time consumption, could be beneficial for applications in these fields. For the specific case of radiation protection in space, the INCL4 model should first be extended to higher energy, in spite of its somehow crude theoretical foundations. Indeed, this model is limited to excitation of the Delta resonance in inelastic nucleon–nucleon collisions. This is largely sufficient for the energy domain relevant for ADS. However, for applications to space missions (and others), this is not satisfactory, since the energy spectrum of Galactic cosmic rays presents a maximum around 0.6 GeV per nucleon, but extends much beyond this domain. It is often considered that accurate simulations require to take account of this spectrum up to 10–15 GeV.

It is the primary purpose of the present work to extend the INCL4 model to this maximum energy. Of course, the addition of the missing inelastic channels is required. This can be done, like in QMD codes, by including resonances with heavier and heavier mass. However, and this is the second motivation of this work, this method may be challenged. Indeed, a rapid scan of the experimental data shows at least fourty non-strange resonances below 2.5 GeV with a width extending from 100 to 500 MeV. The various resonances are so much overlapping that one may wonder whether it is appropriate to consider such objects with a well-defined identity in the course of nuclear reactions. In addition, in view of their large width, considering their propagation as the one of an object with a definite mass in a very short time span may not be very relevant. Furthermore, the interaction of resonances with nucleons and with other resonances is not well known. For these reasons, it looks legitimate to contemplate alternative descriptions in which the explicit resonance degrees of freedom are disregarded or short-cut. In fact, the second purpose of this paper is to investigate the somehow opposite to usual point of view, which consists in considering directly the asymptotically produced particles in nucleon–nucleon collisions and pion–nucleon collisions. Such an approach was already used in Refs. [10,11], in particular for the study of pion-induced reactions, but at low energy (less than 1 GeV). We limit ourselves to produced nucleons and pions in this work. The simulation in the cascade model is implemented by using experimental cross sections for multiple pion production in nucleon–nucleon and pion–nucleon collisions. To make the approach extreme and simple, we first considered that the final particles are generated according to a uniform phase space distribution. Although this

crude choice already gives reasonable results, we preferred to deform the uniform phase space distribution towards a slightly more aligned distribution on the direction of the collisions (in their center of mass). In order to test our ideas, we have performed a comparison of our results with the measurements of the HARP Collaboration [12]. This is actually the third motivation of this work, namely the comparison of our model predictions with an extensive and systematic set of data.

In summary, we want to see in this paper whether the extension of our INCL4.2 model by the adjunction of multipion production as mentioned above is a viable model for applications at high energy, and, for this purpose, to test its predictions against the HARP experimental data. In fact, we want to show that we have devised an effective model, which, in spite of its sometimes uncertain foundations (both for INC in general and for the method of direct pion production in particular) is nevertheless a suitable model to applications in this energy range.

The paper is divided as follows. In Section 2, we shortly present the standard version (INCL4.2) of the Liège intranuclear cascade and the implementation of the inelastic channels mentioned above. Section 3 presents the results and a comparison with experiment, especially with the double differential pion production cross sections measured by the HARP Collaboration. Section 4 contains a discussion of the results. Finally, the conclusion is presented in Section 5.

## 2. The model

### 2.1. A brief description of the INCL4.2 model

We refer to Ref. [4] for a detailed description of the standard version (INCL4.2) of the INCL4 model. It is sufficient here to remind the salient features. The INCL4 model is a time-like intranuclear cascade model. In the initial state, all nucleons are prepared in phase space. Target nucleons are given positions and momenta at random in agreement with a Saxon–Woods and a Fermi sphere distributions, respectively. They are moving in a potential well, describing the nuclear mean field. The incident particle (nucleon or pion) is given the appropriate energy and an impact parameter at random. All nucleons are then set into motion and followed in space–time. They are assumed to travel along straight-line trajectories until two of them reach their minimum relative distance of approach or until a particle hits the nuclear surface. In the first case, the two nucleons can scatter if the relative distance is shorter than the square root of the total particle–particle reaction cross section (at the appropriate energy) divided by $\pi$. The outgoing momenta are then chosen at random in accordance with experimental angular distributions and energy–momentum conservation. In the second case, nucleons are transmitted or reflected, according to their energy and transmission probabilities for plane waves on a potential step. After the possible modification of the motion is applied, straight line motion is resumed until a new possibility occurs, and so on.

Although classical in nature, the model accounts for some quantum aspects: Pauli blocking of collisions, quantum transmission through the nuclear surface, stochastic determination of the final states in nucleon–nucleon (*NN*) collisions and existence of a smooth nuclear mean field. Finally, we want to stress that the model does not include free parameters. There are, of course, parameters such as those characterizing the initial distribution or those entering the procedure for evaluation of the phase space occupancy, but they have been determined once for all. There is no adjustable parameter left to the user.

Although the standard INCL4.2 model is quite successful [4], it has been improved on several points during the last years. We refer to Ref. [13] for a general discussion. However, the extension to high energy is studied here using the standard INCL4.2 model as the starting point, for two main reasons. First, this study has started in parallel with the other developments. Second, many of the other developments, such as the implementation of the cluster production, may have important consequences for transmutation studies, but are of secondary importance here.

## 2.2. Description of multipion production

We give some detail on how the $NN \rightarrow NNn\pi$ process has been implemented. First of all the cross sections $\sigma_T(NN \rightarrow NNn\pi)$ for the production of $n$ pions in a collision between two nucleons in a given isospin state $T$ are constructed, from adjusted parametrizations of experimentally known cross sections for specific final channels, following closely the method of Ref. [14] (we used more data, compiled in Ref. [15], especially at high energy). We constructed explicitly the cross sections up to $n = 3$ and we considered that the rest of the total inelastic cross section (the latter being taken from experiment), corresponds to $n = 4$, which seems reasonable in the energy domain of interest in this paper, at least for the $NN$ collisions. The various cross sections are sketched in Fig. 1.[1]

The simulation of the production of one pion (for $T = 1$), is treated differently from the other channels ($n = 1$ for $T = 0$, and $n \geqslant 2$). In the standard version INCL4.2, the one pion production, in the $T = 1$ channel, results from the following processes

$$NN \rightarrow N\Delta, \quad \Delta \rightarrow \pi N. \tag{1}$$

This is largely sufficient at low incident energy (below ∼2 GeV). Since this dynamics is rather well understood, since the width of the Delta resonance is relatively small and since the $\Delta$ resonance is rather well separated from the other heavier resonances, we decided to keep these processes in our simulations (and the reverse processes for pion absorption). In addition, we simply extended this procedure at higher energy, typically up to $\sqrt{s} = 10$ GeV. As the energy increases, the mass given to the produced $\Delta$ may take large values. To correct for this, we reduce the lifetime of the $\Delta$ by a factor 2 when the mass is larger than 1400 MeV. So, in such cases, the $\Delta$ degree of freedom is then somehow obliterated and the production of one pion is close to a direct production. This procedure provides thus with an intermediate situation between direct pion production and the averaging over resonances heavier than the $\Delta$ resonance. This is admittedly less satisfactory than introducing resonances explicitly, but this preserves the simplicity of our model, which, in our opinion, is essential for applications. As far as utilized cross sections are concerned, the $NN \rightarrow N\Delta$ cross section is identified with the $\sigma_1(NN \rightarrow NN\pi)$ cross section defined above and depicted in Fig. 1. Below $E_{inc} \approx 1.2$ GeV, it reduces to the cross section used in our standard INCL4.2 model. Details can be found in Ref. [4].

For $T = 1$, $n \geqslant 2$ and for $T = 0$, $n \geqslant 1$, the final state is determined as follows. The final momenta of the particles are generated according a slightly modified uniform phase space density. Although the uniform phase space model already gave reasonable results, it does not reflect the so-called peripheralism that characterizes cross sections in this energy regime, namely the fact that the emission of the nucleons is rather forward-peaked around the incident direction [15, 16]. Therefore, we changed the uniform phase space model accordingly. Technically, we used

---

[1] The little bump at the opening of the $T = 0$ channel is an artifact due to a smooth parametrization of scattered and unprecise experimental data.
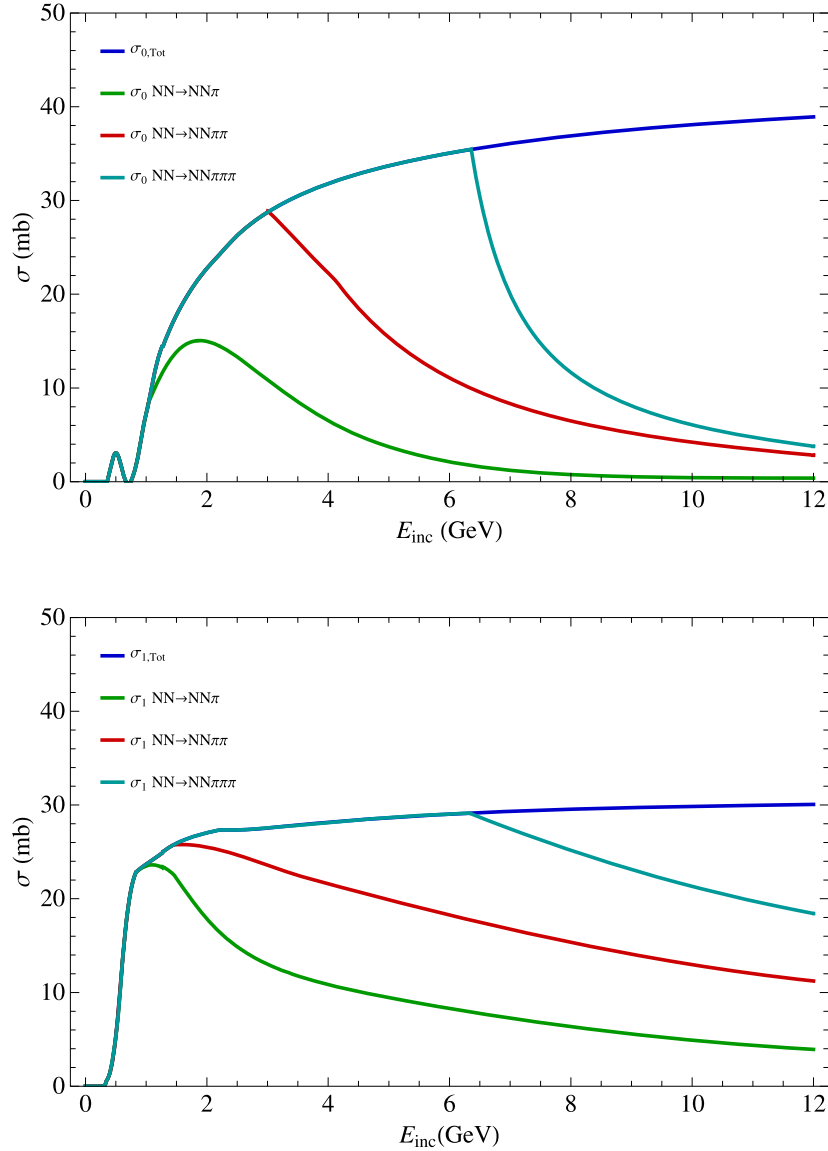
Fig. 1. Total inelastic nucleon–nucleon cross sections in the $T = 0$ (top) and $T = 1$ (bottom), indicated by the upper curves and splitted into 1, 2, 3 and 4 pion production channels, ordered from below. See text and Ref. [19] for detail.

the so-called Raubold–Lynch method [18], and it is then sufficient to bias the two polar angles corresponding to the outgoing direction of the incident nucleon accordingly. Actually, if $\theta$ is the angle between the emission angle of one of the nucleons and its incident direction in the center of mass frame, the distribution of this angle is generated according the following probability law:

$$dP/dt \propto e^{Bt}, \tag{2}$$

where $t$ is the squared momentum transfer of the nucleon and where $B$ is a constant. The value of $B$ has been taken as approximately equal to the slope parameter of elastic scattering and $\Delta$ production angular distributions, which assume a form similar to Eq. (2) (at small angles). The parameter $B$ is slightly dependent upon the c.m. energy. Typically, it is equal to 6 $\text{GeV}^{-2}$ in the energy range under consideration [15–17]. We checked that this model gives a pion emission pattern in $NN$ collisions, that is consistent with the scarce experimental data at our disposal. Of course, pion multiplicities are correct by construction (see above). But we also checked that several observables are correctly reproduced. Details will be given in Ref. [19]. We just show
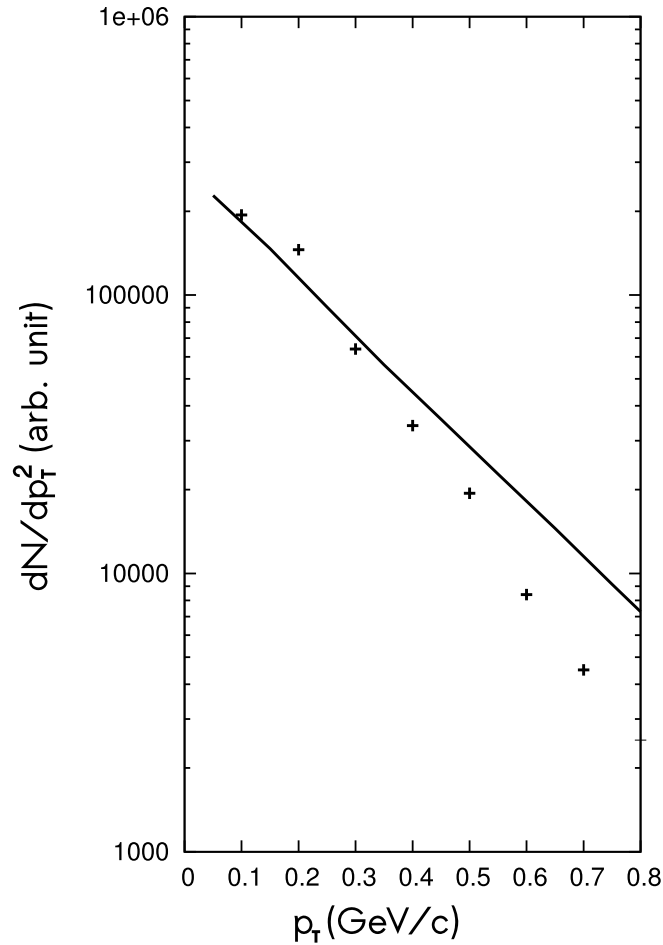
Fig. 2. Squared transverse momentum distribution for positive pions produced in *pp* collisions at incident momentum of 12 GeV/*c*. Data (crosses) from Ref. [21] are compared with our non-uniform phase space model (full line). The two distributions are normalized on the same value at $p_T = 0.1$ GeV/*c*.

here in Fig. 2 the situation for the case of the $p_T$ distribution for positive pions. Our model is able to give a decent picture of the spectrum even for incident momentum as large as 12 GeV/*c*. A comparison with well tested models for *NN* collisions in this energy range, like PYTHIA [20], would also give some indication. We have not done it, because an indirect comparison, at the level of the nucleon–nucleus cross sections, is provided below (see Section 4).

The repartition of the charges among the outgoing particles in the final states is done as follows. For $n = 1$, this is fixed automatically, according to isospin Clebsch–Gordan coefficients. This is true also for $n = 2$, if one assumes that the two pions are in the lowest angular momentum states, which uniquely determines their isospin state. For $n = 3$, we take advantage of the fact that the final states of the three pions can be connected to the final states of two pions with the same charge (with the same initial and final states for the two nucleons): if the three pion state is obtained from the two pion state by the addition of a $\pi^0$ only (like $\pi^+\pi^+\pi^0$ from $\pi^+\pi^+$) the probability for the three pion state is taken equal to the probability for the two pion state; if there are several three pion states which can be connected to a two pion state (like $\pi^+\pi^0\pi^0$ and $\pi^+\pi^+\pi^-$ from $\pi^+\pi^0$) the probabilities for the three pion states are taken as the probability for the two pion state multiplied by 1/3 and 2/3 respectively, which are proportional to the degeneracy of the neutral components ($\pi^0\pi^0$ and $\pi^+\pi^-$). The $n = 4$ states can be connected to the $n = 2$ states by the addition of either a $\pi^0\pi^0$ pair or a $\pi^+\pi^-$ pair. The resulting probabilities

are simply obtained from those of the $n = 2$ case, by multiplication of a factor $1/3$ and $2/3$, respectively. More detail can be found in Ref. [19].

The $\pi N \to Nn\pi$ ($n \geqslant 1$) reactions are treated similarly. The cross sections $\sigma_T(\pi N \to Nn\pi)$ are constructed from the experimental cross sections for definite final states and from the elastic and total $\pi N$ cross sections as parameterized in Ref. [22]. For $n = 1$, the reaction is treated as a $\pi N \to \Delta$ process, with the same mitigation for large masses of the $\Delta$ as the one explained above, so that in practice it corresponds to the $\pi N \to \pi N$ scattering. For $n = 2$–$4$, a similarly modified phase space distribution is used to account for the forward scattering of the pion and the nucleon. We used also a probability distribution with the same form as above (Eq. (2)). However, the values of $B$ are not so well documented as for the $NN$ case. We chose $B = 15\ \mathrm{GeV}^{-2}$, following the indications of Ref. [15]. Distribution of charges for $n = 3$–$4$ is treated in a similar manner as in $NN$ collisions. Pion absorption proceeds to the reverse of the reactions indicated in Eq. (1). It is perhaps a crude approximation and it certainly neglects direct (genuine) absorption on three nucleons. However, the fact that the $\Delta$ may scatter elastically on one, two or more nucleons before disappearing in a $N\Delta \to NN$ reaction takes largely account of the effective pion absorption on three (or more) nucleons. This has been extensively discussed in the frame of the Liège INC model in the past [23,24].

We want to underline that in INCL4.2 and in the modified version just described, the utilized total inelastic $NN$ cross sections are basically the same and are taken from experiment. In the standard version, the only allowed process is the one corresponding to $n = 1$. Therefore, the two versions give the same results for $NN$ collisions if the $n \geqslant 2$ channels are not excited, i.e. for laboratory incident energy (in $NN$ collisions) smaller than ${\sim}1$ GeV (see Fig. 1). For pion–nucleon interactions, there is no excitation of the $n \geqslant 2$ channel in the standard version. So the two models are equivalent for pion incident energy smaller than ${\sim}300$ MeV. We have verified that the two versions of the proton–nucleus numerical code give the same results in nucleon-induced reactions up to incident kinetic energy of the order of 800 MeV.

## 3. Results

### 3.1. Introduction

Since this paper primarily deals with the effect of the description of the inelastic $NN$ collisions, we mainly concentrate here on pion production cross sections, which are the most direct observable linked to this feature. Results relative to the other observables are reserved for a future publication. All our calculations have been run with the adjunction of the version ABLA07 [25] of the ABLA code. The choice of the evaporation code is however of no importance for pion production, since the latter occurs in the cascade stage only.

### 3.2. Total $\pi^+$ and $\pi^-$ yields

We first consider these global observables. Fig. 3 compares the $\pi^+$ and $\pi^-$ yields measured in Ref. [26] and our predictions. Globally the trend for the $\pi^-$ yields are reproduced by the calculations, even if there is some local discrepancy. For the $\pi^+$ yield, there are too few data to draw any definite conclusion, but it seems that the general trend is also well reproduced: at low incident energy, the $\pi^+$ yield is larger than the $\pi^-$ one and the difference decreases with increasing incident energy. The difference decreases also when going from light to heavy targets. These observations are more or less consistent with a production of pions proceeding
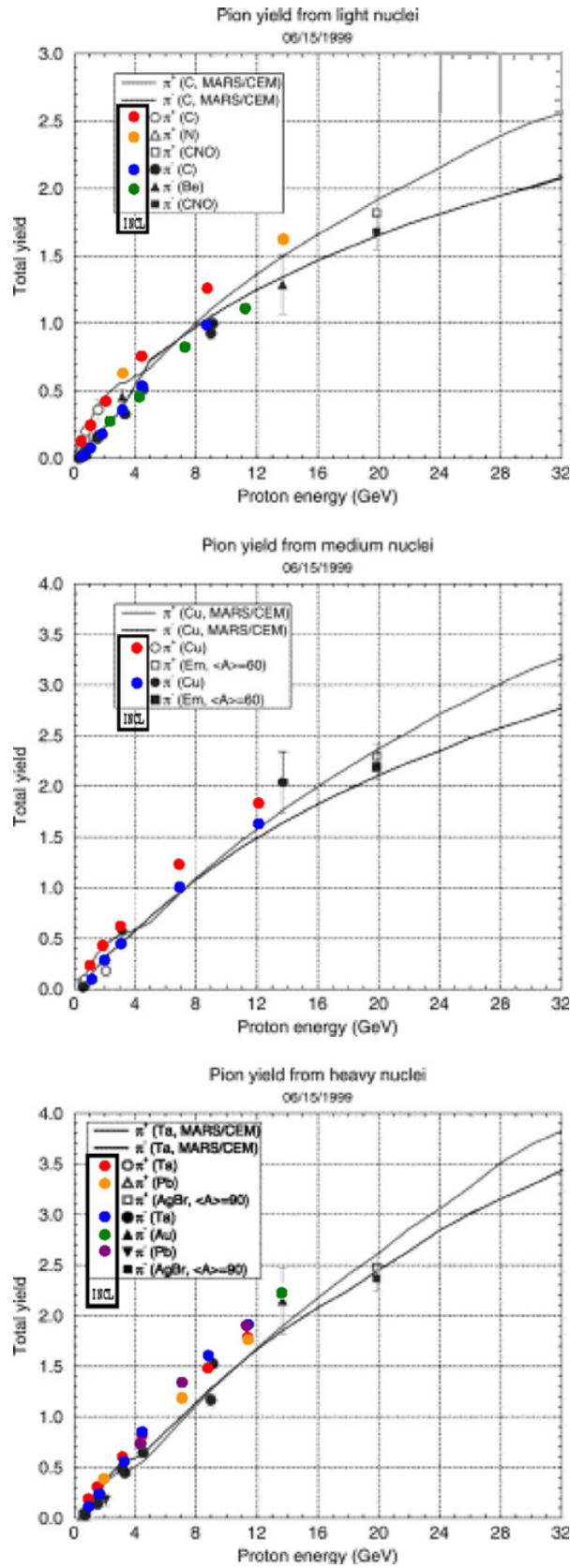
Fig. 3. Total $\pi^+$ and $\pi^-$ yields as functions of the incident energy in proton-induced reactions on light (top), medium-weight (middle) and heavy (bottom) targets. Experimental data are represented by black ($\pi^-$) and open ($\pi^+$) symbols. Our predictions are given by the colored symbols. The meaning of the various symbols can be read from the panels. Data are taken from Ref. [26] and are also compared with the calculations based on the MARS/CEM model, indicated by the full curves.

Fig. 4. $\pi^+$ (left panel) and $\pi^-$ (right panel) production cross sections in proton-induced reactions on several targets and at different incident momenta. The data are obtained by integrating double differential cross sections on the acceptance (in angle and momentum) of the HARP experiment. The experimental data correspond to the open symbols and our predictions correspond to the black symbols (lines are just to guide the eye). Data are from Refs. [30–33] and refer to Be, C, Al, Cu, Sn, Ta and Pb targets.

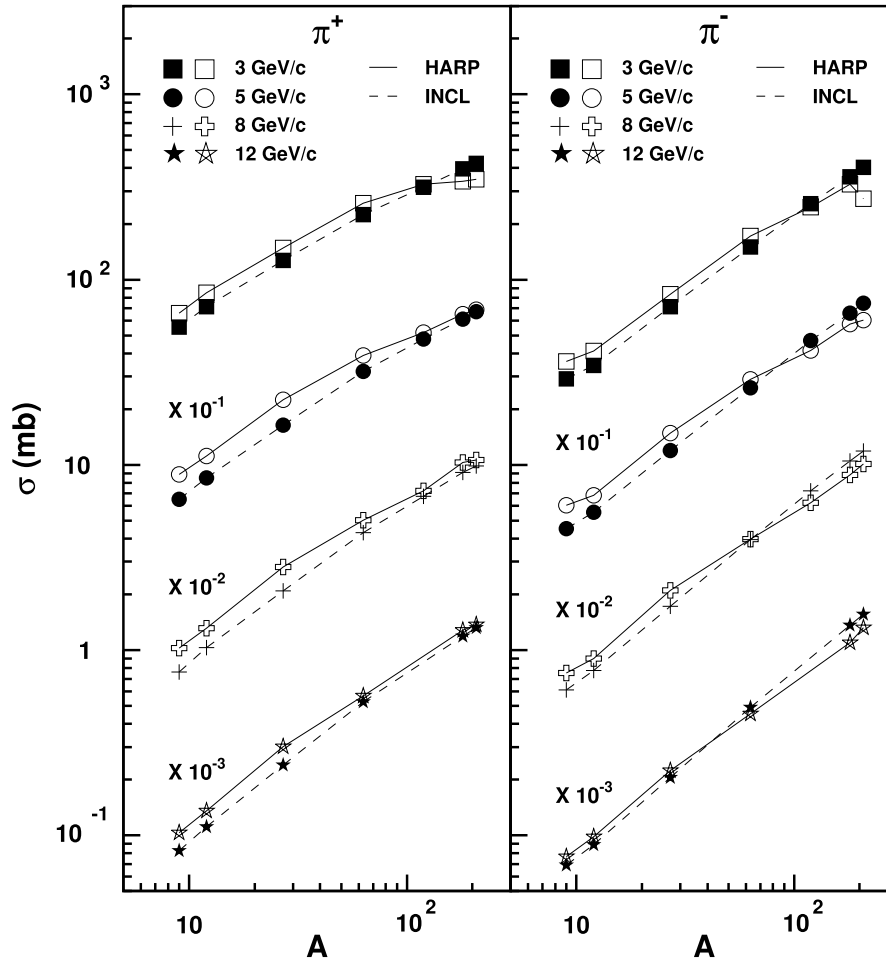through few collisions at low incident energy and involving more and more collisions when the target mass increases and/or when the incident energy increases. Fig. 3 gives also a comparison with calculations using on the MARS/CEM model, based on Refs. [27–29]. The results are very similar to ours.

Fig. 4 shows integrated $\pi^+$ and $\pi^-$ cross sections, measured by the HARP Collaboration [12] for different targets and different incident energies. We have to specify from the beginning that the experimental points correspond in fact to the integrated double differential cross sections over the acceptance of the experimental set-up. The latter corresponds to a domain extending from 350 to 2150 mrad for the polar angle and from 150 to 400–750 MeV/$c$ (depending upon the angles) for the pion momentum. This acceptance roughly corresponds to 25% of the total production cross section.

One can see that, on the average, the general trends are reproduced: the production cross sections are increasing with the target mass with roughly a power law $\sigma = \sigma_0 A^\alpha$. The exponent $\alpha$ is close to unity for $\pi^-$ production. For $\pi^+$ production, it goes from 0.7 for the lowest incident energy to 0.9 for the highest one. The fact that $\alpha$ exceeds $2/3$, the black disk value, is also an indication of a pion production resulting from many collisions. The comparison with our results
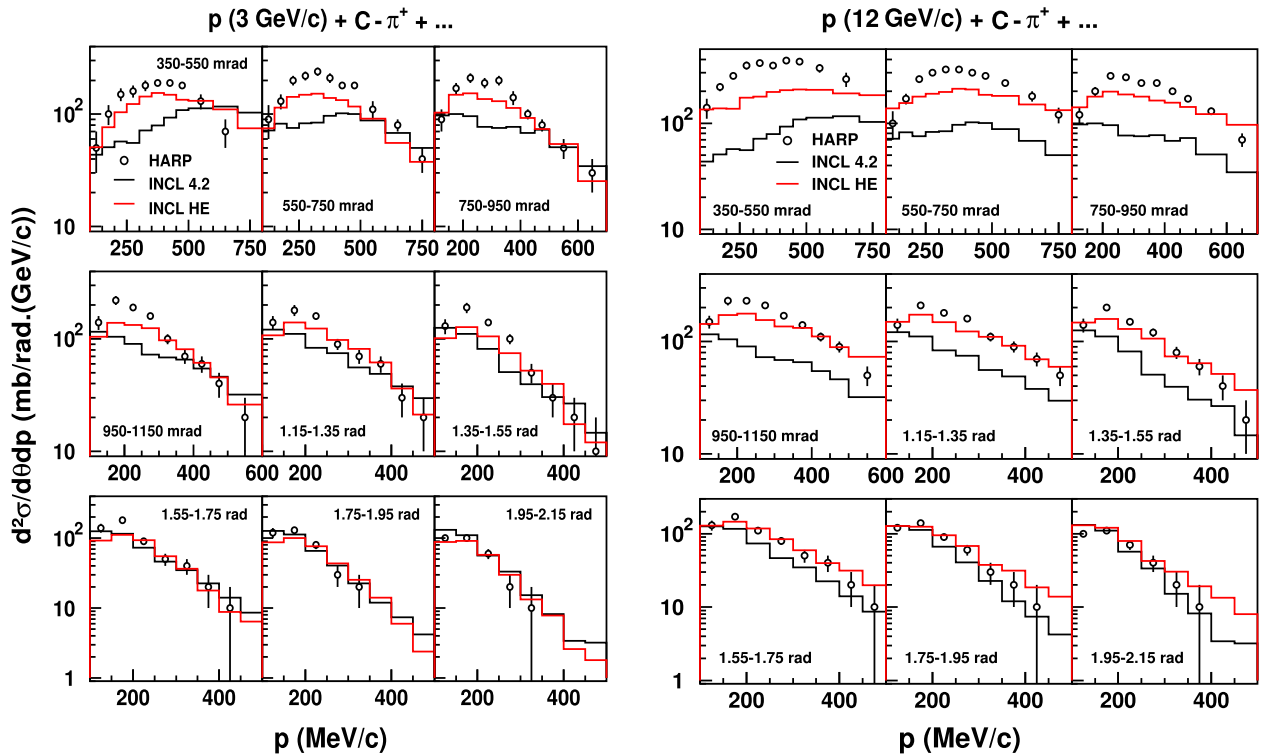
Fig. 5. Double differential cross sections for the production of positive pions in proton-induced reactions on C at 3 GeV/$c$ (left) and at 12 GeV/$c$ (right) incident momentum. Data (symbols) from Refs. [30,33] are compared with the standard version (black lines) and the improved version (red lines) of the INCL4 model (standard INCL4.2 version plus implementation of direct multipion production). See text for detail. (For interpretation of the references to color in this figure legend, the reader is referred to the web version of this article.)

show that the model slightly underestimates the production cross section for light targets, at least at low incident energy.

The dependence of the cross sections upon the incident energy (not shown) is slightly slower than linear and is roughly reproduced by our calculations. However, the cross sections do not increase very much over the incident energy range for light targets, whereas they change by a factor 3 for heavy targets (both for $\pi^+$ and $\pi^-$). The behavior for light targets contrasts with the one indicated in Fig. 3: in that case, the total production cross section (equal to the yield multiplied by the total reaction cross section, which does not change much above 2 GeV/$c$) is increasing with energy, by a factor 2–3, in the energy range under interest here. The difference likely comes from the rather restricted acceptance for the data collected in Fig. 4, especially in momentum space: energetic pions produced in light targets, which are more numerous as the incident energy increases, are missing in these data.

### 3.3. Double differential cross sections for proton-induced reactions

Double differential cross sections for $\pi^+$ production in proton-induced reactions on three targets at two incident momenta (3 and 12 GeV/$c$), measured by the HARP Collaboration, are presented and compared with our calculations in Figs. 5–7. In order to exhibit the effect of the implementation of direct multipion production, we show the results with both the standard version INCL4.2 and the improved version (from now on, "improved version" stands for the standard version INCL4.2 plus the implemented multipion production) of our model. Of course, calculations has been done for all targets and many incident momenta between 3 and 12 GeV/$c$, but
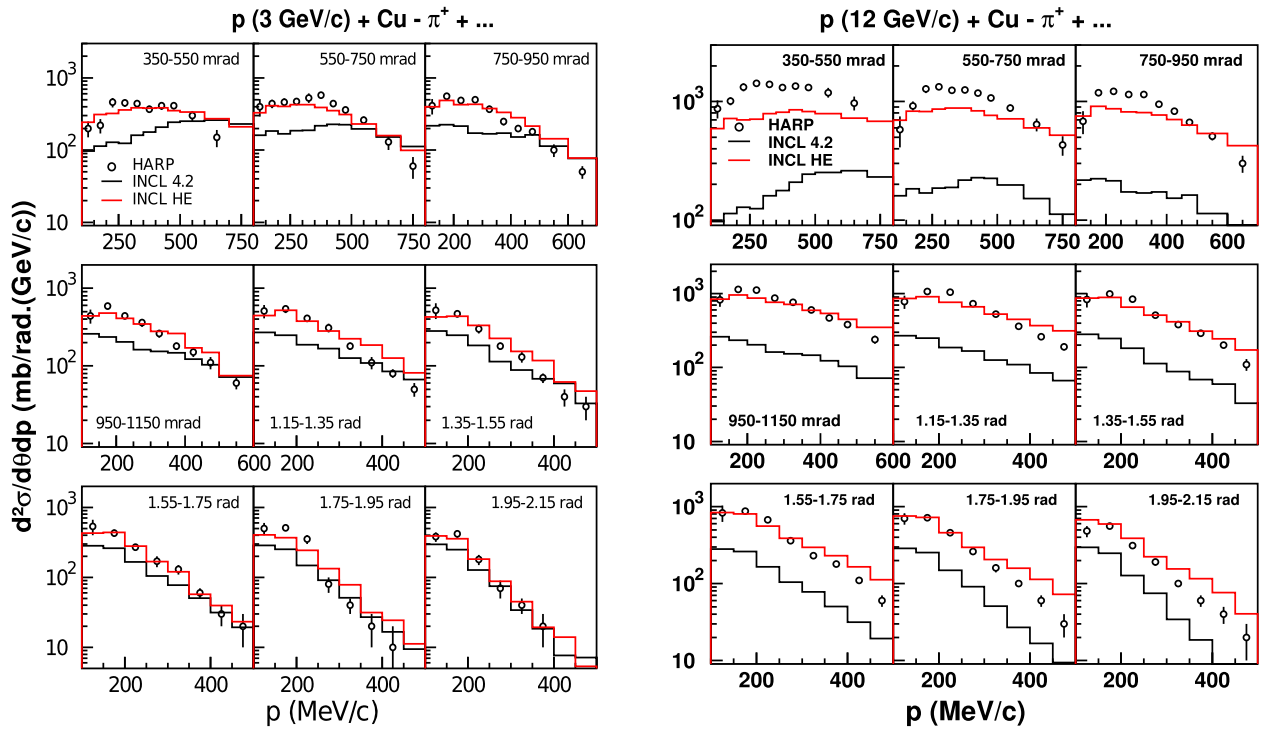
Fig. 6. Double differential cross sections for the production of positive pions in proton-induced reactions on Cu at 3 GeV/$c$ (left) and at 12 GeV/$c$ (right) incident momentum. Data (symbols) from Refs. [30,33] are compared with the standard version (black lines) and the improved version (red lines) of the INCL4 model. See text for detail. (For interpretation of the references to color in this figure legend, the reader is referred to the web version of this article.)



Fig. 7. Double differential cross sections for the production of positive pions in proton-induced reactions on Pb at 3 GeV/$c$ (left) and at 12 GeV/$c$ (right) incident momentum. Data (symbols) from Refs. [31,33] are compared with the standard version (black lines) and the improved version (red lines) of the INCL4 model. See text for detail. (For interpretation of the references to color in this figure legend, the reader is referred to the web version of this article.)

Fig. 8. Same as Fig. 5 for the production of negative pions. Data from Refs. [30,33].

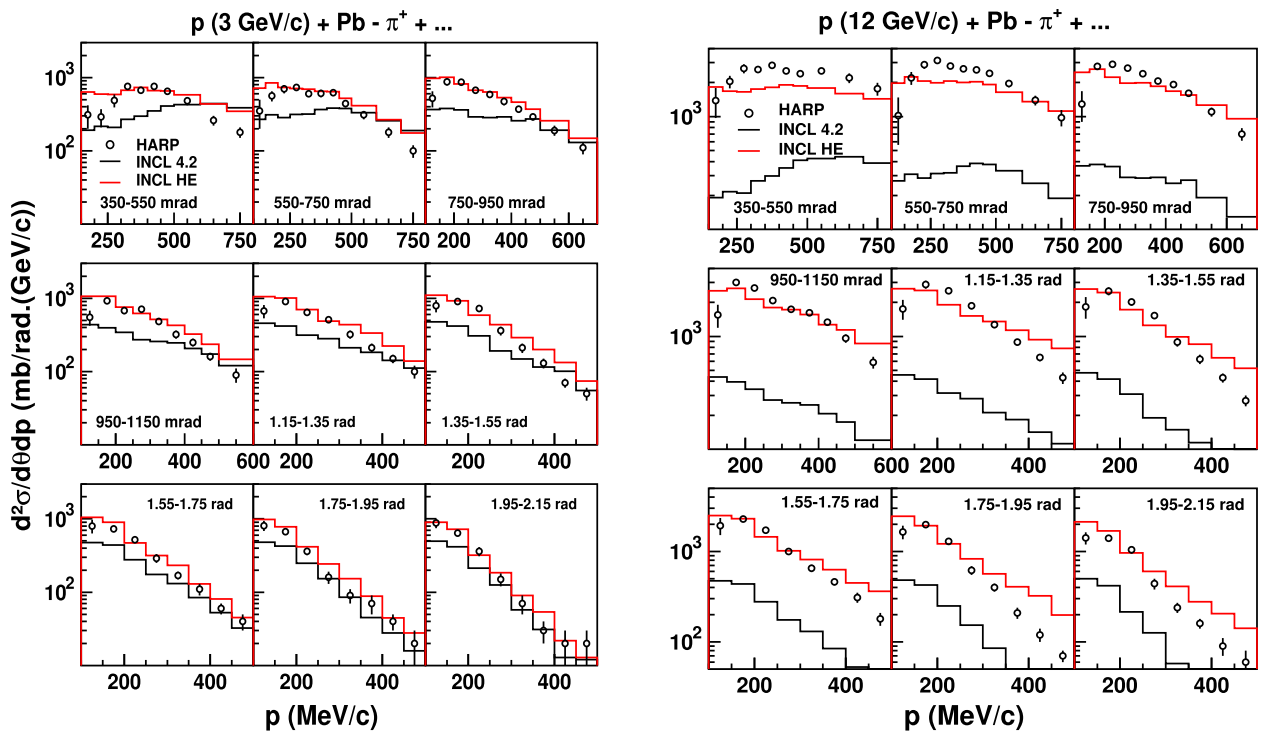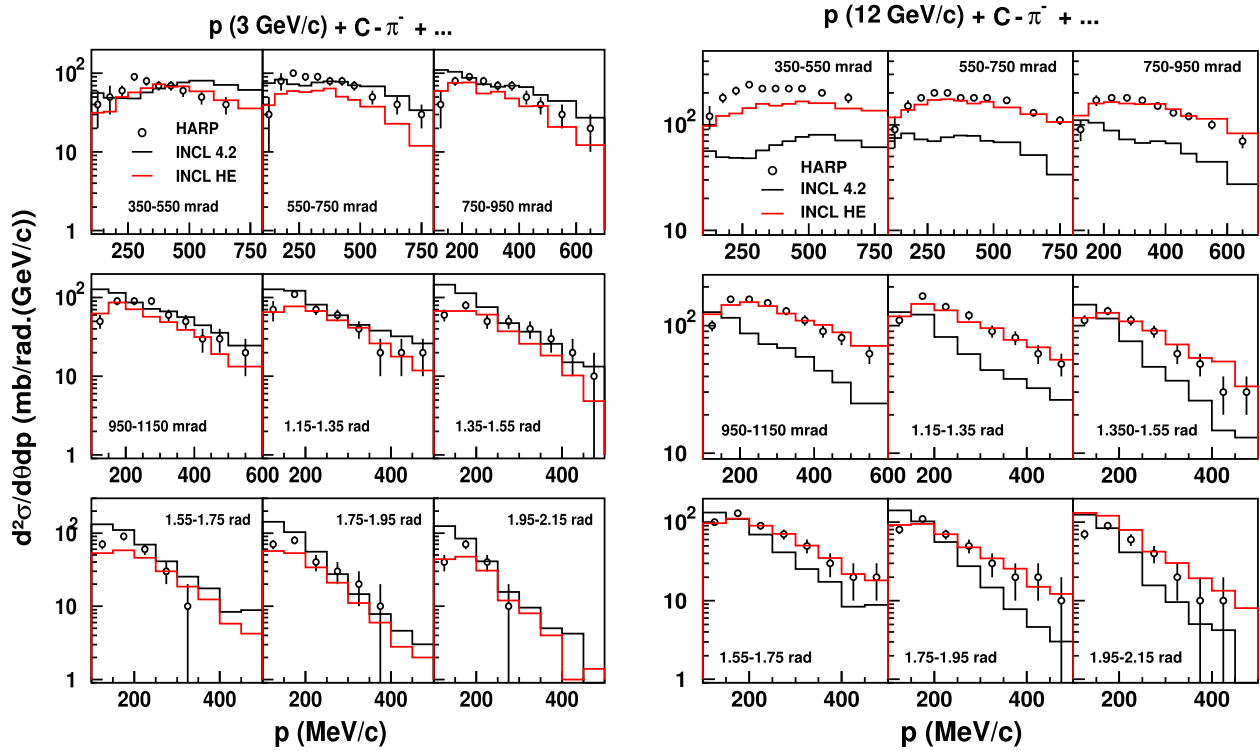the results shown are sufficient for illustrating the general trends of our results. One can say that, on the average, the agreement is quite remarkable, though not perfect. Our results systematically underestimate the cross sections at small angles for the highest incident momenta. This shortcoming seems to decrease with increasing target mass. One can detect also a slight overestimate of the cross sections at large angle and large pion momentum.

Figs. 8–10 display the same comparison for $\pi^-$ production. In this case, our predictions are even slightly better. Another relatively small shortcoming appears for Pb at 12 GeV/$c$: the yield for low energy pions at small angles is overestimated.

The shapes of the pion momentum spectra do not change very much over the whole set displayed in Figs. 5–10. They show a maximum at small angles for all cases and smoothly change to a basically exponentially decreasing curve at large angles. The maximum is less and less pronounced with increasing incident momentum and with increasing target mass. This is basically in agreement with a multiple scattering picture. Indeed, this scenario is expected to produce more and more pions in the forward direction as the incident energy increases and, to some extent, when the target size increases.

The absolute values of the production cross sections are also smoothly changing with the parameters: angle bin, momentum bin, target mass and incident momentum. For otherwise fixed conditions, the cross sections are increasing with the target mass. They are increasing with the incident energy, more for heavy targets than for light targets, in agreement with what is said in Section 3.2. This increase is less pronounced at large angles than at small angles. Finally the $\pi^-$ production cross sections are smaller than the $\pi^+$ production cross sections, and this is more pronounced for light targets and low incident momentum. This is once again consistent with the multi scattering picture. Indeed, it is expected that an incident proton has a higher chance to produce a $\pi^+$ than a $\pi^-$ in a single collision on a nucleon, taken as a neutron or a proton with equal probability, because it brings an extra positive charge. This effect is slightly weakened for
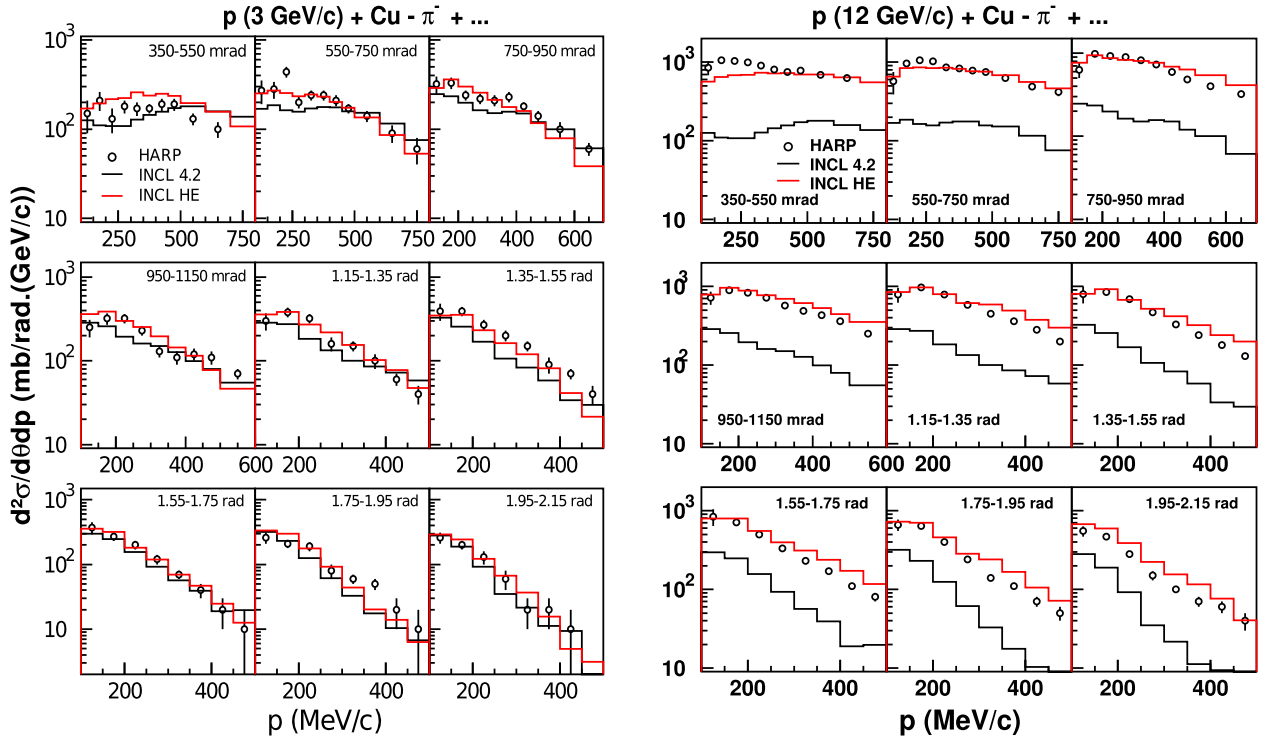
Fig. 9. Same as Fig. 6 for the production of negative pions. Data from Refs. [30,33].
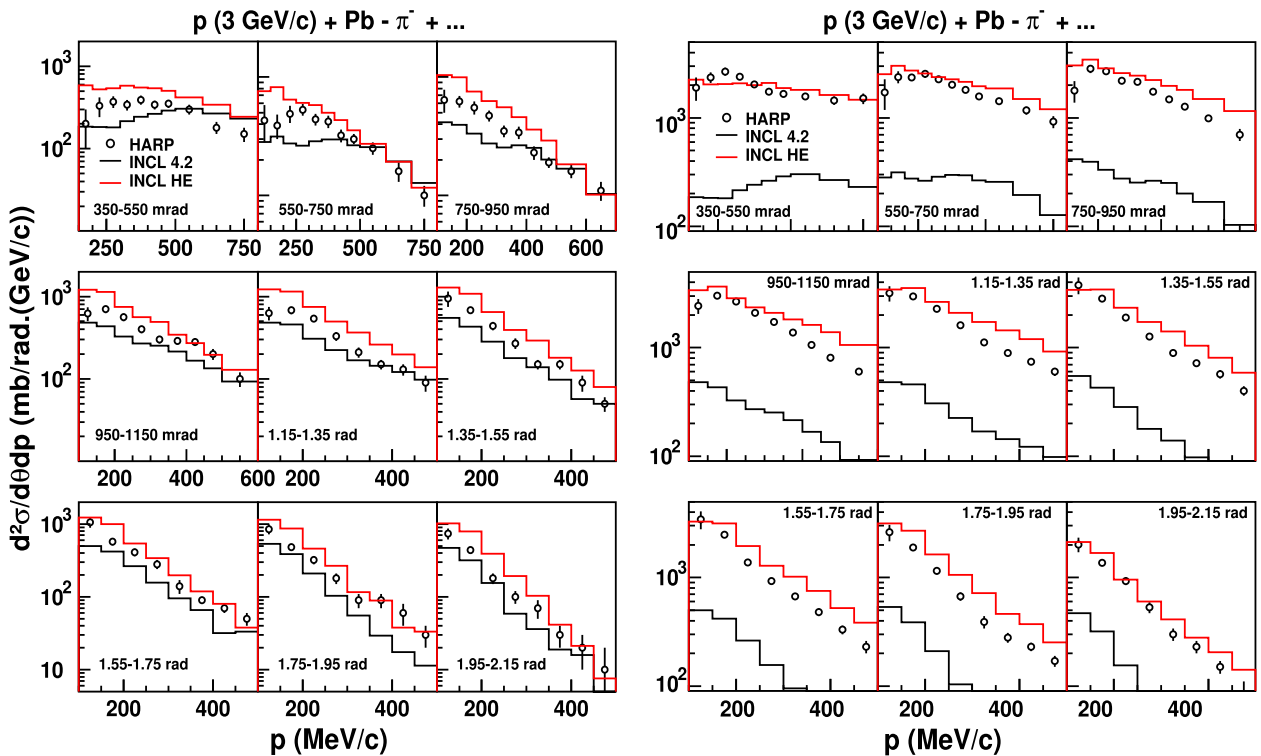


Fig. 10. Same as Fig. 7 for the production of negative pions. Data from Refs. [31,33].

heavy nuclei, which are more neutron rich. This tendency to produce positive pions is attenuated by multiple collisions, i.e. when the incident energy and/or the target mass are increasing.

It is interesting to notice that our model, even if it does not perfectly reproduce the data, has nevertheless caught the general trends of the shape and intensity of the pion spectra. This

presumably means that it properly describes the multiple scattering in detail and that the latter, in reality, is dictated by the free elementary cross sections, as this is the basic premise of our INCL4 model.

In Figs. 5–10, we have included the predictions of the standard INCL4.2 model. First of all, one can see that the modifications described above have tremendously improved the predictive power of the model. It is interesting to note that the predictions of the modified model and those of the standard model are rather close to each other at large angles and for low incident momentum. We recall that in the standard model, the main source of pions is coming from $NN \to N\Delta$, $\Delta \to \pi N$ processes. Of course, pions may be absorbed and re-emitted, but without changing very much the yield [34]. Therefore, this strongly suggests that, at large angles and low incident energy, pions are basically produced by a small number of collisions, in agreement with the discussion above.

The HARP Collaboration has recently published data [35] on pion production at very forward angles and for a larger range of pion momentum than in their previous works. We show some results in Fig. 11, along with our predictions. In order not to multiply the figures only the comparison at 12 GeV/$c$ is shown, but it is illustrative of all the incident momentum range, from 3 GeV/$c$ to 12 GeV/$c$ (more detail in Ref. [19]). One can see that the agreement is largely satisfactory and that our model for multipion production is able to generate high momentum pions. Actually, the calculated spectra do not fall off sufficiently fast at high pion momentum, compared to the experimental data. This may indicate that our modified uniform phase space model is still a little bit too crude. It seems that the configurations producing pions with the highest momentum should have a somehow reduced weight. Nevertheless, these results show at least that the production of pions by approximately uniform phase space does not produce results in sharp disagreement with experimental data.

### 3.4. Double differential cross sections for pion-induced reactions

In Figs. 12 and 13, we compare the HARP data concerning pion production in pion-induced reactions on Cu with the predictions of our improved model (we do not compare here with the standard INCL4.2 model, since the inelastic $\pi N$ cross section vanishes in this version). Actually, we only show the results at 5 GeV/$c$, but they are illustrative of the kind of agreement that is achieved in the whole range of incident momentum. Grossly speaking, the agreement is not as good as for proton-induced reactions (compare with Figs. 6 and 9). Nevertheless some general features are well reproduced, such as the shapes of the spectra, which are flatter than in the proton-induced case and the variations of the absolute value of the cross sections with varying angle and when going from positive pion production to negative pion production. But the deficiencies observed in the proton-induced case, namely the underprediction at small angles (at least for $\pi^-$ production) and the overestimate of the cross sections at large momentum for large angles, are enhanced in the pion-induced case. We are inclined to attribute these shortcomings to a lack of a sufficiently forward-peaked pion production in pion–nucleon collisions. We remind that we biased the pion production in the forward direction for the first pion only (and the nucleon), but not for the other pions in $\pi N$ collisions producing several pions.

Fig. 13 indicates that our theoretical results are clearly better for a heavy target. This is a general observation for all our results. This probably points to a limitation of the neglect of the resonance degrees of freedom, which, of course, should manifest themselves more importantly in light target, for which the large surface/volume ratio compensates a short lifetime more easily. This may as well indicate that multiple scattering is important for heavy targets and that the
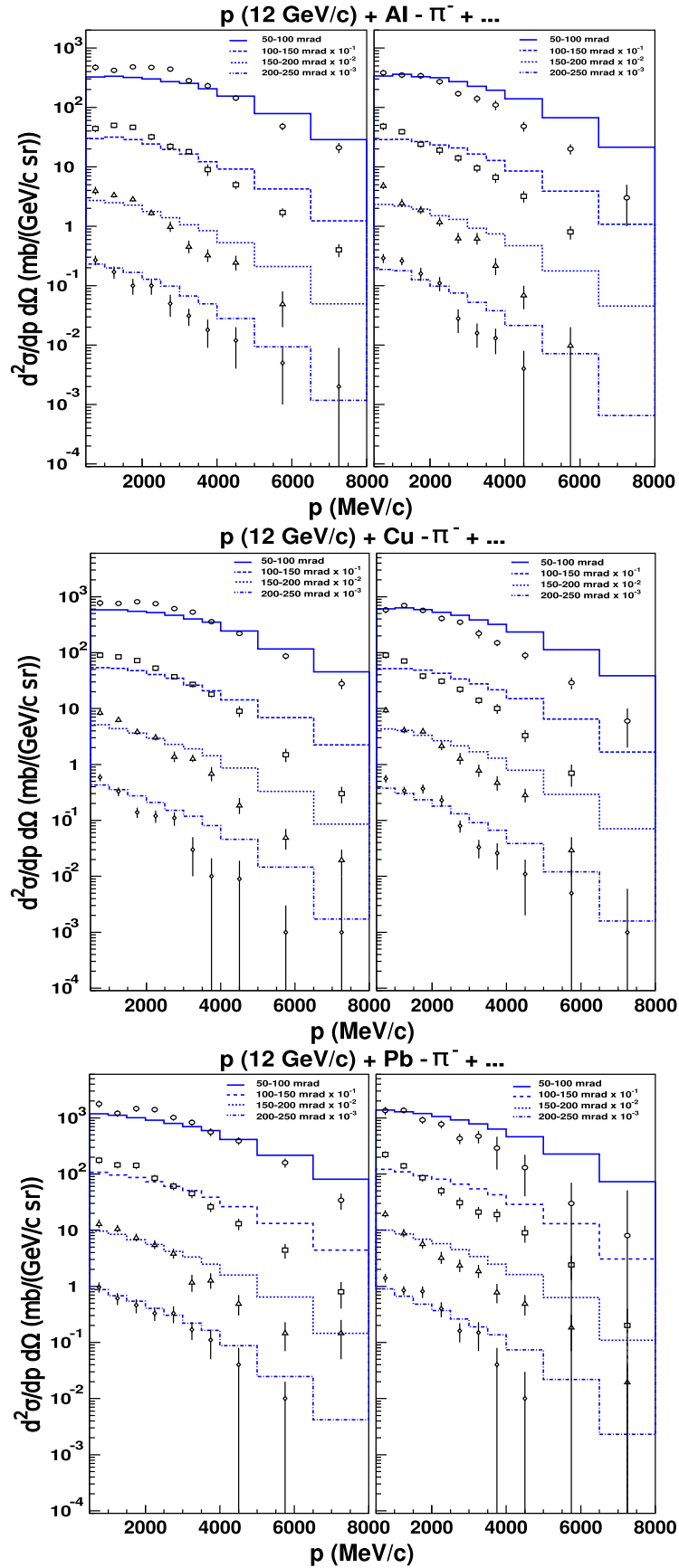
Fig. 11. Double differential cross sections for the production of positive (left) and negative (right) pions in proton-induced reactions on Al, Cu and Pb (from top to bottom) at 12 GeV/$c$ incident momentum. Data (symbols) from Ref. [35] are compared with the improved version of the INCL4 model (histograms). See text for detail.
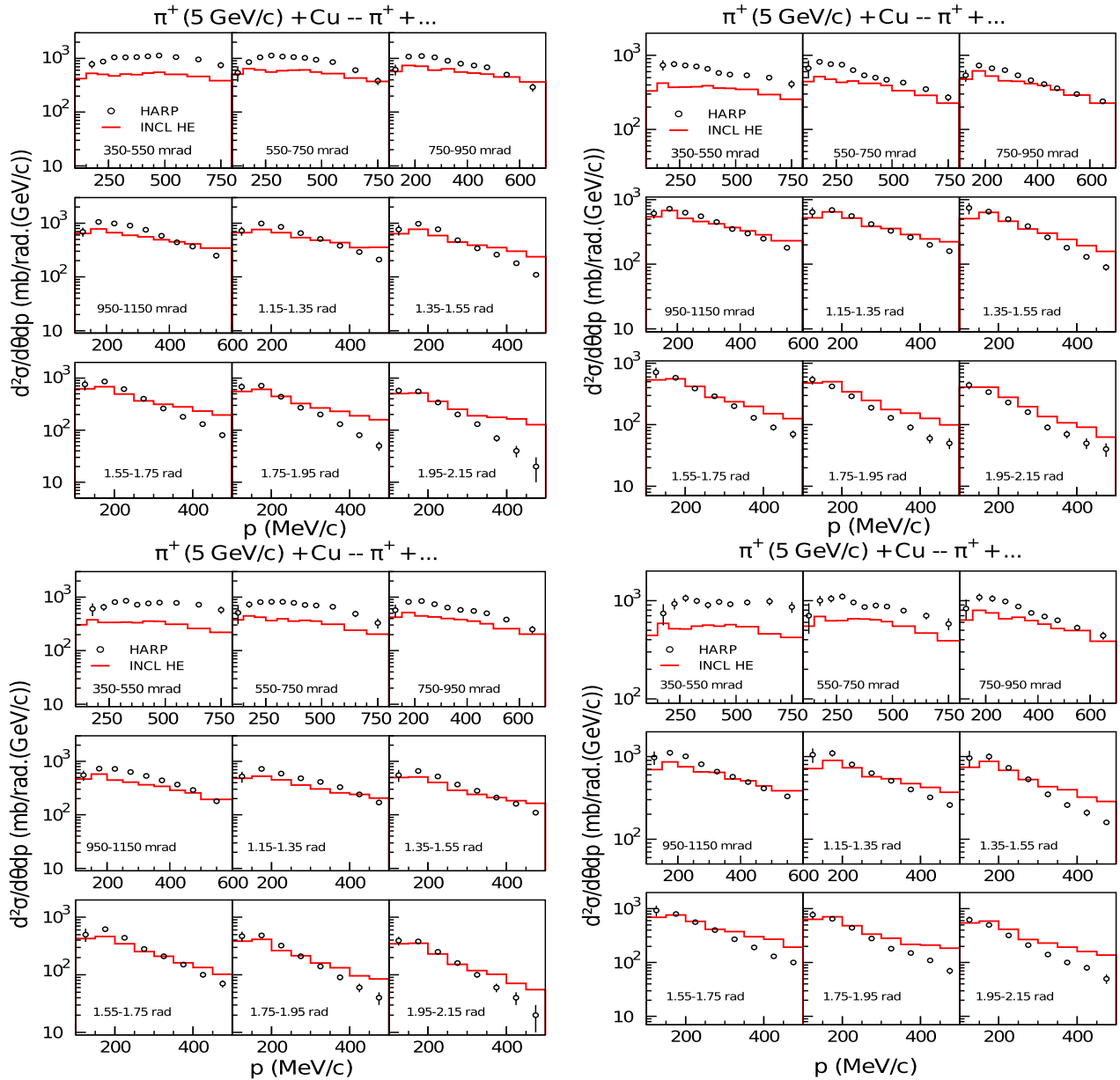
Fig. 12. Double differential cross sections for the production of positive (left column) and negative (right column) pions in reactions on Cu nuclei induced by positive (first row) and negative (second row) pions at 5 GeV/$c$ incident momentum. Data (symbols) from Ref. [36] are compared with the improved version of the INCL4 model. See text for detail.

results are then less sensitive to the detail of the elementary cross sections. Nonetheless, in order to achieve a good agreement in such cases, it is important to have a good balance between single and multiple scattering. And, accordingly, our results indicate that our model of direct multiple pion production in $NN$ and $\pi N$ collisions is at least guaranteeing such a good balance, which, we think, is not an obvious result.

## 4. Discussion

The main purpose of our work was to extend the INCL4.2 model for spallation reactions up to 10–15 GeV incident energy and to test it on systematic data for proton-induced reactions. There are not so many good quality data on proton production or on residue production. We

Fig. 13. Same as Fig. 12 for Pb target.

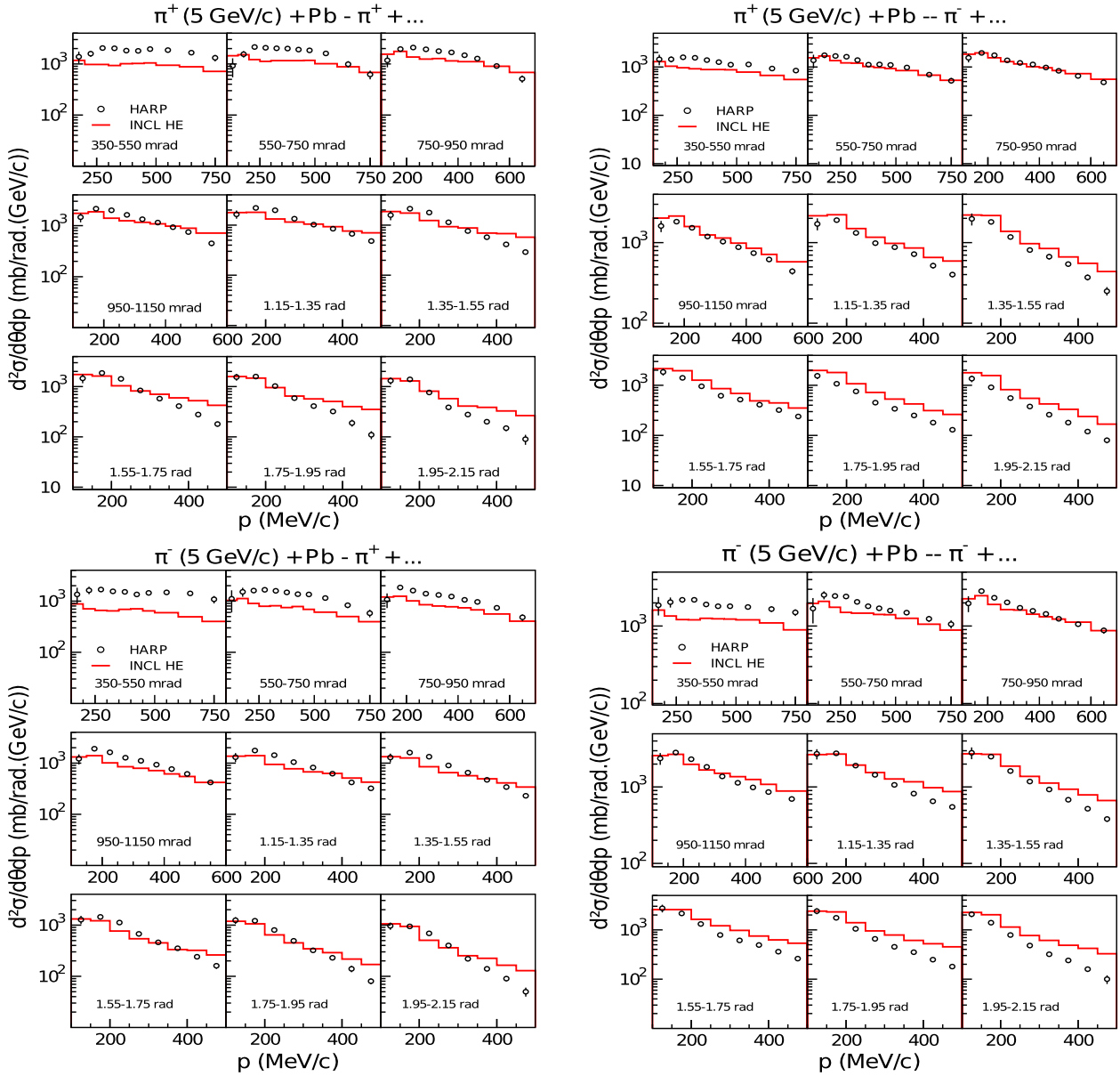found reasonable agreement for a few existing data concerning proton production we compare with. Results will be published in Ref. [19]. In the present paper, we concentrated on the comparison with very detailed and systematic data on pion production produced in the last years by the HARP Collaboration. The main modification of the INCL4.2 model consists in introducing multipion production both in $NN$ and $\pi N$ collisions. The detail of the modification has been inspired from $NN$ and $\pi N$ cross section phenomenology. The total pion production cross sections were taken equal to the experimental total inelastic cross sections, when they are known. Other cross sections, like the total $\pi^0$–$n$ cross sections and the cross section for particular channels, have been obtained from the data following the method of Ref. [14], which tries to exploit the isospin symmetry as far as possible. A model for the generation of the final states is nevertheless needed, as we explained, and the features of this model were chosen as simple as possible. For the generation of the final energy and momentum of the particles, we considered the simplest departure from uniform phase space model, allowing forward peaking for the final direction of the incoming particles (this is also the simplest technical modification of the method of Ref. [18]).

In the extension of INCL4.2 proposed in this paper, inelastic channels other than pure pion-producing channels have been neglected. The most important ones are the strangeness production channels. But, the neglect of strangeness production is not expected to be important in the energy range under consideration, except, of course, for specific strangeness production channels. First, strangeness production in *NN* collisions remains low (at least one order of magnitude compared to non-strange production) in this energy range [37]. Second, calculations, based on QMD, indicate that, in proton–nucleus collisions in the same energy range, strange particle cross sections are at least one order of magnitude smaller than non-strange particle cross sections [38,39].

We have shown that the simple extension of INCL4.2 described above is able to give a reasonably good description of pion double differential cross sections in a whole range of incident momentum extending from $\sim 2$ GeV/$c$, where the validity of the standard version still holds, to $\sim 12$ GeV/$c$, and for targets ranging from Be to Pb. Of course, the agreement is not perfect, but the degree of global agreement gives confidence in the validity of our model, at least in its predictive power. We recall that there is no adjustment parameter in this model and that its simplicity allows for some refinements.

Let us analyze in some detail the level of agreement for proton-induced reactions. As far as global quantities, yields (Fig. 3) or integrated cross sections (Fig. 4), are concerned, the agreement is very good. On the average, the experimental data are reproduced within 10%, with maximum departure lying around 20% (see Fig. 4). But the repartition of the produced pions, embodied by double differential cross sections, shows larger disagreements. Some systematic features are revealed. Generally, the cross sections are underestimated at low pion momentum and small angle and are overestimated, to a smaller extent, at large pion momentum and large angle. In general, the level of disagreement decreases with increasing target mass. For $\pi^+$ production the agreement has a tendency to decrease with excitation energy, whereas for $\pi^-$ production the agreement is slightly increasing with excitation energy. We want to mention that these discrepancies are enhanced when we used a full uniform phase space model (not shown). This leads us to believe that the departure from uniform phase space that has been introduced in inelastic *NN* and $\pi N$ collisions is not yet large enough. We remind that only the final direction of the incoming particles is biased. A biased emission of the other pions toward forward peaking, as suggested by experiment [21] (see also Fig. 2), would presumably improve our results. This requires however a more substantial modification of the Raubold–Lynch method. More or less the same considerations apply to pion-induced reactions.

We would like to mention that our results reproduce some other general trends. For instance, the ratio of the $\pi^-$ to $\pi^+$ cross sections (in proton-induced reactions) lies about 1/3 at forward angles and moves slowly to 1/2 at large angles for light targets. For heavy targets, these numbers are roughly 1/2 at forward angles and 1 at large angles. As incident energy increases, the ratio is coming slowly close to unity, almost reached at 12 GeV/$c$. Other results of similar kind are also observed in pion-induced reactions. The fact that these trends are reproduced in our calculations means that we have a good model for the repartition of the charges in *NN* and $\pi N$ pion-producing collisions and a good model for $\pi N$ interaction.

We have shown in this work that a description based on the direct multipion production picture gives a valuable alternative to the conventional approach based on the usual hadronic resonance picture (see below for a detailed comparison). Several considerations can be made. First there is no obvious indication in the data under consideration here of the manifestation of the resonance degrees of freedom. Pion spectra have smooth shapes and change slowly with angle, target mass and incident energy. Even if resonances are formed, it is not really expected to clearly see their fingerprint in inclusive data. Pion production spectra are presumably more resulting

from the propagation of the pions produced in the first collisions through the target nucleus than indicative of a source (including resonances) more or less at rest. This was already noticed in antiproton annihilation on nuclei [40,41], which presents a similar situation and a similar average number of pions. More exclusive measurements are probably necessary to exhibit the possible formation of resonances. Two particle correlations (involving a pion and a nucleon for instance) are probably not very useful, because a peak corresponding to a resonance in the invariant mass spectrum is superposed to a huge background of uncorrelated pairs. A careful analysis of such correlations for the $\Delta$ resonance in proton–nucleus reactions, made in Ref. [42], showed that the signal is barely visible, in light nuclei only, in the energy range under consideration. It is thus expected, and this is underlined in Ref. [42], that neglecting resonance formation by assuming direct pion production can affect only the calculations of this kind of quantities in light nuclei. This conclusion is presumably even more valid for broader resonances. Our work seems to indicate that, as far as exclusive measurements are concerned, our approach appears to be as good as the resonance approach (except for light nuclei), although the two approaches seem, at first sight, mutually exclusive. One is thus led to admit that there is some kind of duality of these two approaches, for inclusive quantities. This may not be surprising, as a very large width for a resonance means that the degree of freedom attached to its presence is more or less obliterated.

Although our main goal was a test of the proposed extension of the INCL4.2 model, based on direct multipion production picture, we want to say a few words about works similar to ours and devoted to the description of pion production in the 2–12 GeV/$c$ incident momentum range. The HARP data have been extensively compared with the MARS [27–29] and Geant4 [43] code systems in various references [33,35,36,26]. These code systems possess a high flexibility, in particular in the choice of the physics model for the reaction mechanisms. It is not surprising therefore that they generally reach a better agreement with experimental data than our work. Roughly speaking, in many cases, the discrepancies are a factor 2 or more lower than in our case. However, the fact that these code systems use different reaction models for different domains of energy, as underlined in Ref. [39], sometimes introduces some unphysical jumps in the excitation functions of total pion production. See Ref. [44] for a discussion. We want also to emphasize that the Fluka code system [46,45] also gives very good results for the comparison with the HARP Collaboration [47,48], owing also to the flexibility of this code system and perhaps to a better choice of the main reaction model.

The comparison with the work of Ref. [39] is perhaps more meaningful, since both this work and ours test a single reaction model, the GiBUU model [49] in Ref. [39] and INCL4 + ABLA in our work. Both models are equally successful, although the agreement reached in Ref. [39] is better in many cases. Both models suffer from similar shortcomings, such as an overestimate of the pion spectrum at large momentum and large angle.

As we explained at long, the main difference between the two works comes from the explicit introduction of the resonance degrees of freedom which is replaced in our work by the direct multipion production. This is not however the only difference. For instance, in the GiBUU model, the resonance dynamics is replaced smoothly by a string dynamics (as embodied in the PYTHIA event generator), starting from $\sqrt{s} \sim 2.5$ GeV. Incidentally, this gives us some confidence of the validity of our modelization of the nucleon–nucleon and pion–nucleon interactions in the energy range considered here, at least once again in the frame of our approach (results for inclusive cross sections, non-strange channels, etc.). Interestingly also, the work of Ref. [39] introduces reduced cross section for hadrons during hadronization times after collisions. In our case, free cross sections are used everywhere. Finally, we want to stress that there is no free parameter in our work and that phenomenological parameters, like nuclear radius and the $B$ parameters intro-

duced in Section 2, have been fixed on known phenomenology. This may contrast with the work of Ref. [39], in which many parameters, such as resonance–resonance cross sections, are not constrained by phenomenology. Let us however mention that these parameters have been constrained by a longstanding work of comparison with data for a wide range of nuclear reactions, in particular in heavy-ion physics.

## 5. Conclusion

In this paper, we have improved the INCL4.2 model in order to extend its domain of validity in incident energy, which was limited to 2 GeV, because inelastic elementary processes were limited to the $\Delta$ excitation. But, at the same time, we have also tested the direct multipion production picture, which offers an alternative to the usual resonance excitation picture. This new approach is motivated by the larger and larger number of broad overlapping resonances in the baryon mass spectrum when c.m. energy is increasing. In this paper, we have reported on the results of this new approach by taking advantage of the possibility of comparing with a large set of data concerning pion production in the 2–12 GeV energy range, provided by the HARP Collaboration. We have shown that, despite its simplicity, our approach gives rather good agreement with experimental data, comparable with, but slightly less good than, the one achieved by transport code systems. The success of our approach indicates than there seems to exist a kind of duality between the direct multipion production picture and the resonance picture, at least as far as inclusive quantities are concerned. Finally, because our extension of the INCL4.2 does not have free parameters, its successes are rather encouraging and open the possibility of having an even more reliable model with further improvements.

## Acknowledgements

## References

[1] W. Gudowski, Nucl. Phys. A 654 (1999) 436c.
[2] R.G. Vassil'kov, V.I. Yurevich, in: Proc. of ICANS-11, KEK Report 90-25, 1991, p. 340.
[3] J.-C. David, et al., A new benchmark of spallation models, IAEA Reports, in press; see also: http://www-nds.iaea.org/spallations/.
[4] A. Boudard, J. Cugnon, S. Leray, C. Volant, Phys. Rev. C 66 (2002) 044615.
[5] J.-J. Gaimard, K.-H. Schmidt, Nucl. Phys. A 531 (1991) 709.
[6] A.R. Junghans, et al., Nucl. Phys. A 629 (1998) 635.
[7] I.S.K. Gardner, in: S. Myers, et al. (Eds.), EPAC98: Proceedings, IOP Publishing, 1998, p. 98.
[8] M. Durante, Riv. Nuovo Cimento 25 (8) (2002) 1.
[9] E. Parker, Space Weather 3 (2005) S08004.
[10] E. Hernãndez, E. Oset, Nucl. Phys. A 455 (1986) 584.
[11] L.L. Salcedo, E. Oset, M.J. Vicente-Vacas, C. Garcia-Recio, Nucl. Phys. A 484 (1988) 557.
[12] M.G. Catanesi, et al., HARP Collaboration, The HARP detector at the CERN PS, Nucl. Instrum. Meth. A 571 (2007) 527.

[13] J. Cugnon, A. Boudard, S. Leray, D. Mancusi, in: Proc. of Int. Topical Meeting on Nuclear Research Applications and Utilization of Accelerators (AccApp09), IAEA, Vienna, 2010, ISBN 978-92-0-150410-4, SM/SR-02, http://www-pub.iaea.org/MTCD/publications/PDF/P1433_CD/datasets/abstracts/sm_sr-02.html.

[14] J. Bystricky, P. La France, F. Lehar, F. Perrot, T. Siemiarczuk, P. Winternitz, J. Physique 48 (1987) 1901.

[15] A. Baldini, V. Flaminio, W.G. Moorhead, D.R.O. Morrison, Landolt-Börnstein New Series, Group 1, vol. 12a, Springer, Berlin, 1988.

[16] G.J. Igo, Rev. Mod. Phys. 50 (1978) 523.

[17] J. Cugnon, D. L'Hôte, J. Vandermeulen, Nucl. Instrum. Meth. B 111 (1996) 215.

[18] E. Raubold, G.R. Lynch, Their event generator has not been published by the authors; it has been described by F. James in "Monte Carlo Phase Space", Lectures Series CERN 68-15, May 1968.

[19] S. Pedoux, PhD thesis, University of Liège, unpublished.

[20] T. Sjöstrand, S. Mrenna, P. Skands, PYTHIA 6.4 Physics and Manual, FERMILAB-PUB-06-052-CD-T Report, 2006.

[21] V. Blobel, et al., Nucl. Phys. B 69 (1974) 454.

[22] Th. Aoust, J. Cugnon, Phys. Rev. C 74 (2006) 064607.

[23] J. Cugnon, M.-C. Lemaire, Nucl. Phys. A 489 (1988) 781.

[24] J. Cugnon, P. Deneye, J. Vandermeulen, Nucl. Phys. A 500 (1989) 701.

[25] A. Kelić, M.V. Ricciardi, K.-H. Schmidt, in: D. Filges, et al. (Ed.), Joint ICTP-IAEA Advanced Workshop on Model Codes for Spallation Reactions, IAEA INDC (NDS)-1530, IAEA Publications, Vienna, Autriche, 2008, pp. 181–222.

[26] J. Collot, H.G. Kirk, N.V. Mokhov, Nucl. Instrum. Meth. A 451 (2000) 327.

[27] N.V. Mokhov, The MARS Code System User Guide, Version 13(95), Fermilab-FN-628, 1995.

[28] N.V. Mokhov, et al., MARS Code Developments, LANL Report LA-UR-98-5716, 1998, nucl-th/9812038v2, 16 December 1998, http://www-ap.fnal.gov/MARS/.

[29] S.G. Mashnik, A.J. Sierk, in: T.A. Gabriel (Ed.), Proceedings of the Fourth Workshop on Simulating Accelerator Radiation Environments (SARE4), Knoxville, ORNL, 1999, p. 29.

[30] M.G. Catanesi, et al., HARP Collaboration, Eur. Phys. J. C 53 (2008) 177, arXiv:0709.3464 [hep-ex].

[31] M.G. Catanesi, et al., HARP Collaboration, Eur. Phys. J. C 54 (2008) 37, arXiv:0709.3458 [hep-ex].

[32] M.G. Catanesi, et al., HARP Collaboration, Eur. Phys. J. C 31 (2007) 787, arXiv:0706.1600v1 [hep-ex].

[33] M.G. Catanesi, et al., HARP Collaboration, Phys. Rev. C 77 (2008) 055207, arXiv:0805.2871.

[34] Th. Aoust, PhD thesis, University of Liège, 2007, unpublished.

[35] M. Apollonio, et al., HARP Collaboration, Phys. Rev. C 80 (2009) 035208.

[36] M. Apollonio, et al., HARP Collaboration, Phys. Rev. C 80 (2009) 065207.

[37] Z. Chen, Int. J. Modern Phys. E 2 (1993) 285.

[38] J. Aichelin, Phys. Rep. 202 (1991) 233.

[39] K. Gallmeister, U. Mosel, Nucl. Phys. A 826 (2009) 151.

[40] J. Cugnon, in: J.-M. Richard, E. Aslanidès, N. Boccara (Eds.), The Elementary Structure of Matter, Springer-Verlag, Berlin, 1988, pp. 211–218.

[41] J. Cugnon, P. Jasselette, J. Vandermeulen, in: C. Amsler, et al. (Eds.), Physics at LEAR with Low-Energy Antiprotons, Harwood Ac. Publ., Chur, 1988, pp. 775–778.

[42] M. Trzaska, et al., Z. Physik A 340 (1991) 325.

[43] Geant4 Collaboration, Geant4 – a simulation toolkit, Nucl. Instrum. Meth. A 506 (2003) 250.

[44] A. Bolshakova, et al., Eur. Phys. J. C 70 (2010) 543.

[45] G. Battistoni, S. Muraro, P.R. Sala, F. Cerutti, A. Ferrari, S. Roesler, A. Fassò, J. Ranft, in: M. Albrow, R. Raja (Eds.), Proceedings of the Hadronic Shower Simulation Workshop 2006, Fermilab, 6–8 September 2006, AIP Conf. Proc. 896 (2007) 31.

[46] A. Fassò, A. Ferrari, J. Ranft, P.R. Sala, FLUKA: a multi-particle transport code, CERN-2005-10, 2005, INFN/TC-05/11, SLAC-R-773.

[47] F. Ballarini, et al., AIP Conf. Proc. 769 (2005) 1197.

[48] G. Battistoni, et al., Recent developments in the FLUKA nuclear reaction models, in: Proc. 11th Int. Conf. on Nuclear Reaction Mechanisms, Varenna, Italy, June 12–16, 2006.

[49] http://theorie.physik.Physik.uni-giessen.de/GiBUU, cited in Ref. [39].